

A CFD Analysis of Gas Plume Stratification in Confined Space

Xinsheng Jiang, Biao He, Qiang Liu*, Dong Wang, Jiannan Xu, Wei Xie

Army Logistics University of PLA, Chongqing 401311, China
(13251364337@163.com)

Abstract

Numerical simulation of gas plume stratification was carried out using the method of large eddy simulation (LES). The gas plume model based on LES, the control equations and the numerical calculation method were analyzed and the application of LES in multicomponent gas plume simulation was explored. In this paper, the model was validated by the experimental data of helium leakage in a confined environment [1-2] Then, the model was used to simulate the stratification behavior of the gasoline vapor plumes in a confined environment. The calculated results show that the components in gasoline vapor show different stratifying laws within 240s. In relation to air, the denser components tend to stay at the 20% lower part of the space, while the lighter ones prefer to disperse in the 80% upper part of the space. This study may provide key parameters and serve as a reference to related engineering design for oil depot hazard monitoring and early warning.

Key Words

Large-eddy simulation (LES), Gas plume, Stratification characteristics, CFD.

1. Introduction

Gas plume stratification refers to the vertical density gradient [2] generated when partial air components of different density flow under the action of buoyance, such as the stratification behavior of the oil in a leakage accident in a confined space. The plume and its stratification are different from the fully developed turbulence and is generally with lower Reynolds number. There are the turbulent motion, laminar motion and the transition area of the two in the flow. Therefore,

the traditional turbulence model is no longer applicable [3], and the large eddy simulation (LES) has become the preferred choice for simulating the gas plume motion [4-5].

LES is an extremely promising method to simulate complicated turbulent, which makes up the shortcoming of direct numerical simulation (DNS), i.e. heavy calculation burden and the shortcomings (low resolution ratio and poor universality) of Reynolds-averaged Navier–Stokes Simulation (RANS). The advantages of LES are as follows: Its requirement for spatial resolution is much less than the direct numerical simulation method; under the existing computational conditions, it is possible to simulate more complex flows with higher Reynolds numbers; it can obtain more turbulence information than RANS, such as large-scale velocity and pressure pulsation. These dynamic information is of great significance to the natural environment and engineering design [6-7]. With the development of computer technology, since the 1990s, LES has gradually become a hot topic in numerical simulation of turbulence. Many commercial software have also added large eddy simulation modules, such as FDS (fire dynamics simulator). It is a kind of flame dynamics software combining LES and DNS and used to simulate the low speed and hot drive flow. At present, LES has been widely applied in the flow in the atmospheric boundary layer, wake flow of wind turbine, solar troposphere, combustion and sound field simulation.

This paper takes the oil vapor as the research subject, and a LES-based numerical simulation model of gas plume stratification features is proposed, which solved the problems of the discreteness of the control equations, meshing and time discreteness. The spatial and temporal distribution of different gas components are obtained.

2. Numerical Simulation Model of Gasoline Vapor Plume Stratification Based on Large Eddy Simulation

The solving thought of LES is to only calculate the large-scale pulsation in turbulence numerical simulation, but to establish the model of the influence of small-scale pulsation. Therefore, the large eddy simulation involves how to achieve the separation of large-scale vortices and small-scale vortices and how to close the filtered control equations.

Under isothermal conditions, the gas motion is controlled only by the continuous equation and the momentum conservation equation, which are expressed as follows respectively:

Momentum conservation equation:

$$\frac{\partial \rho u_i}{\partial t} + \frac{\partial \rho u_i u_j}{\partial x_j} = -\frac{\partial p}{\partial x_i} + \mu \frac{\partial^2 u_i}{\partial x_j \partial x_j} + \rho g_i \quad (1)$$

Continuous equation:

$$\frac{\partial \rho}{\partial t} + \frac{\partial \rho u_i}{\partial x_i} = 0. \quad (2)$$

where: ρ refers to the temperature of the mixed gas, t refers to the time, u stands for the speed, p is the pressure, μ is the dynamic viscosity, and g is the gravity acceleration. $i = 1, 2, 3$ and $j = 1, 2, 3$ refer to the corresponding direction of the component.

In the multi-component gas composed of gasoline vapor and air, the components are subject to the law of conservation of mass, respectively. The convection-diffusion equation is:

$$\frac{\partial}{\partial t}(\rho Y_\alpha) + \frac{\partial}{\partial x_j}(\rho Y_\alpha u_j) = -\rho D_{\alpha,m} \frac{\partial Y_\alpha}{\partial x_j} \quad (3)$$

where: Y_α is the mass fraction of the α^{th} component in the mixture; $D_{\alpha,m}$ is the mass diffusion coefficient for the α^{th} component.

2.1 Filtering Function Based On Large Eddy Simulation

In the LES model, the filtering function is introduced to realize the separation of the vortexes of different size. The filtering expression of the flow variable is:

$$\bar{\Phi}(x) = \int_D \Phi(x') G(x; x') dx' \quad (4)$$

where: $\bar{\Phi}$ refers to the filtered flow variable, D refers to the fluid domain, and G is the filter function limiting the small-scale vortex.

After formula (1) and (2) are processed by the filter function, the following equations can be obtained:

$$\frac{\partial \bar{u}_i}{\partial t} + \frac{\partial \bar{u}_i \bar{u}_j}{\partial x_j} = -\frac{1}{\rho} \frac{\partial \bar{p}}{\partial x_i} + \frac{\mu}{\rho} \frac{\partial^2 \bar{u}_i}{\partial x_j \partial x_j} + g_i + \frac{\partial \tau_{ij}}{\partial x_j} \quad (5)$$

$$\frac{\partial \bar{u}_i}{\partial x_i} = 0 \quad (6)$$

where: the dash line above the character indicates the amount after filtering; $\tau_{ij} = \overline{u_i u_j} - \overline{u_i} \overline{u_j}$ means the sub-grid-scale stress, which is not closed. The construction of the closed model of the sub-grid-scale stress is one of the key problems in realizing large eddy simulation.

After (3) is processed by the filtering function, the following equation can be obtained:

$$\frac{\partial \overline{Y}_i}{\partial t} + \overline{u_j} \frac{\partial \overline{Y}_i}{\partial x_j} = D_{i,m} \frac{\partial^2 \overline{Y}_i}{\partial x_j^2} + T_j \quad (7)$$

This equation is a mass fraction conservation equation, where: $T_j = \overline{u_j Y_i} - \overline{u_j} \overline{Y_i}$ refers to the flux of the sub-grid mass fraction, which is also not closed. Since the sub-grid turbulence mass flux has little effect on the total turbulence mass flux [8], the sub-grid mass fractional flux term is omitted here.

2.2 Subgrid Model

The subgrid model is established to keep the control equation closed. The sub-grid stress based on the eddy viscosity model can be expressed as:

$$\tau_{ij} = 2\nu_{sgs} \overline{S}_{ij} + \frac{1}{3} \delta_{ij} \tau_{kk} \quad (10)$$

where: ν_{sgs} refers to the sub-grid turbulence viscosity; \overline{S}_{ij} refers to the deformation rate of the solvable scale; δ_{ij} stands for the unit tensor component; the isotropic part τ_{kk} in the stress can be included into the item of pressure, so only the modeling of ν_{sgs} is needed.

The dynamic Smargorinsky-Lilly model dynamically obtains the coefficient of the sub-grid model through the information of the large vortex velocity field, but requires an explicit filtering to obtain local turbulence information, which consumes more computation time than the algebraic model. The WALE model has the same advantages as the dynamic Smargorinsky-Lilly model, which can dynamically figure out the coefficients of the sub-grid model through the information of the large vortex velocity field, realize the automatic adjustment of different flow patterns, capture the transition from laminar flow to turbulence, and meet the requirement of flow field simulation of the complicated flow of gas plume in a limited room without the need for explicit filtering, significantly reducing the amount of calculation. Therefore, this paper chooses the WALE model as the sub-grid model for the gas plume stratification simulation in limited space.

2.3 Numerical format

The use of a central difference scheme in LES can reduce the diffusion of convective terms [9], but the limitation is that it may produce an unbounded value, i.e. when the Peclet number is greater than 2, there will be false upper and lower spikes. Even so, the bounded condition of the center difference in LES (Peclet number is less than or equal to 2) does not have to be strictly satisfied [10]. However, when the temperature and quality are involved, unbounded values are of no physical meaning, and bounded center differential schemes must be used. Therefore, in the model established in this paper, the convection scheme of the continuous equation and the momentum conservation equation is the central difference scheme, and the convective scheme of the mass conservation equation is a bounded center difference scheme.

In the time format, the first order format is like the first-order upwind space difference scheme, which is easy to produce large numerical diffusion, and is generally used in the turbulence equation. The second order backward Euler format does not have a strict time step limit, which can be applied to the calculation of both regular time step and variable time step. But as with the second-order convection scheme, it is easy to produce unbounded results. Thus, the time format of the mass fraction conservation equation should be set to a bounded second order format.

The time step can be calculated according to the pulsation frequency of the airflow. A pulse period should contain 10 to 20 time steps [11]. The pulsation frequency can be determined by the number of Strouhal [12]:

$$Sr = \frac{lf}{v} \quad (11)$$

where: l refers to the fluid characteristics length; f refers to the pulse frequency; and v refers to the flow rate.

The Strouhal number in the plume flow can be expressed as:

$$Sr = 0.8Ri^{0.38} \quad (12)$$

where Richardson number $Ri = \frac{[\rho_{\infty} - \rho_{plume}]gD}{\rho_{\infty}U^2}$; $Ri =$; ρ_{∞} and ρ_{plume} refer to the environmental fluid and plume density respectively.

3. Calculation and Analysis of Stratification Characteristics of Gasoline Vapor Plume in Restricted Space

The LES model was established to analyze the characteristics of the stratifying behavior of gasoline vapor plume in a leakage in a confined space. The volatile components of the gasoline mainly include isobutane (9.6%), isopentane (17.2%), hexane (16%), and a small amount of light components, such as methane and ethane [13]. Because the kinematic characteristics of the gasoline vapor plume are mainly related to buoyancy, this paper chooses isobutane with the density greater than air and methane with the density smaller than air as the research object.

The ideal research scene shall house a lot of equipment, with natural ventilation or forced ventilation conditions, as well as a large number of liquid fuel leakages or natural evaporation of gasoline vapor. However, such a complex scenario has a strong dependence on the geometry of the space and the circumstances under consideration. In contrast, the study of very simple situations is the very useful first step for discovering the basic laws involved. Therefore, the abovementioned geometric model is adopted to study the stratification rules of the gasoline vapor after leakage.

Assume that the gasoline vapor enters the confined room at the leakage rate of 1NL/s, and the leakage event continued for 240s [14]. The physical parameters of the gas under the condition of 300K and 1atm are shown in Table 1.

Tab.1. Main Physical Parameters of The Gas

Gas	density /(kg·m ⁻³)	Dynamic viscosity /(kg·m ⁻¹ ·s ⁻¹)	Isoelectric heat capacity/ (J·kg ⁻¹ ·K ⁻¹)	Diffusion coefficient in air/(m ² ·s)	Molecular weight
Air	1.176 0	17.35 × 10 ⁻⁶	1 005	\	28.966
He	0.162 6	19.90 × 10 ⁻⁶	5 193	0.658 × 10 ⁻⁴	4.003
Methane	0.652 8	11.25 × 10 ⁻⁶	2 228	0.196 × 10 ⁻⁴	16.043
Isobutane	2.432 6	7.67 × 10 ⁻⁶	1 670	0.131 × 10 ⁻⁴	58.120

The distribution of the global turbulence scale of the fluid domain calculated using the k-ε model of RANS is shown in Figure 1. The figure shows that the overall turbulence scale near the wall is relatively small (around 0.074m) and the minimum value appears only near the inlet and outlet. Except for this, most of the scale is more than 0.178m. Therefore, the initial grid is re-divided according to the ratio of 1/12. The scale of the grid far from the wall surface is adjusted to 0.0184m, and that of the grid near the wall surface is adjusted to 0.0062m, which is shown in Figure 2.

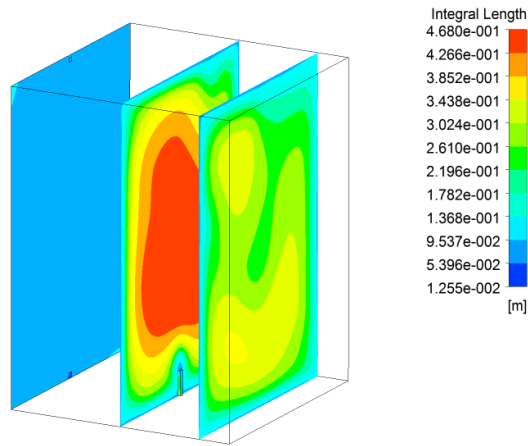


Fig.1. Integral Turbulence Length Scale

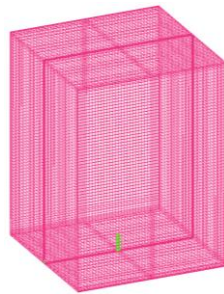
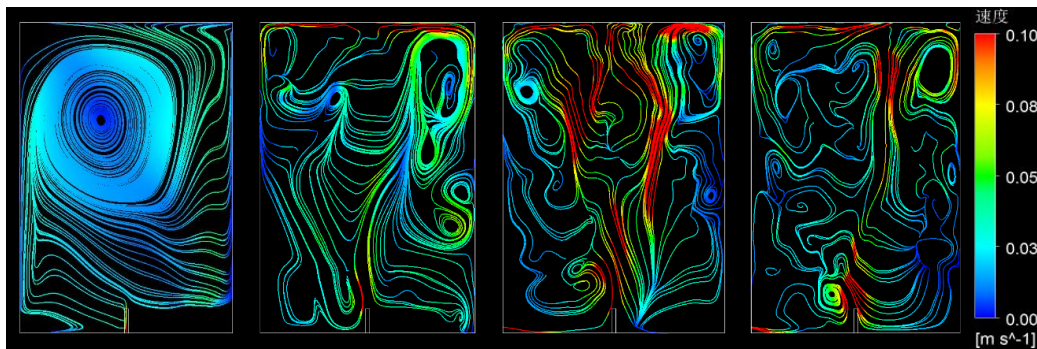


Fig.2. Grid After Refinement

The flow field development pre-calculated using LES is shown in Figure 3. The 0s corresponding flow field is the RANS steady-state calculation results. It can be seen that the RANS steady-state results are far from satisfying the needs, and the LES pre-calculation is favorable to the formation of airflow vortex. At 120s, the vortex of the flow field has formed, so it serves as the initial flow field for LES calculation.



(a) 0 s

(b) 40 s

(c) 80 s

(d) 120 s

Fig.3. Development of Flow Field with Prior Les. Streamlines Are Shown on The Mid-Plane of The Room Colored with The Velocity Magnitude

The simulation results for isobutane and methane leakage are shown in Figure 4. The movement rules of two components after gasoline leakage can be seen: isobutane mainly presents a distribution close to the bottom and begins to accumulate from the bottom; methane begins to move upwards and quickly disperses most of the space and fills the space from top to bottom.

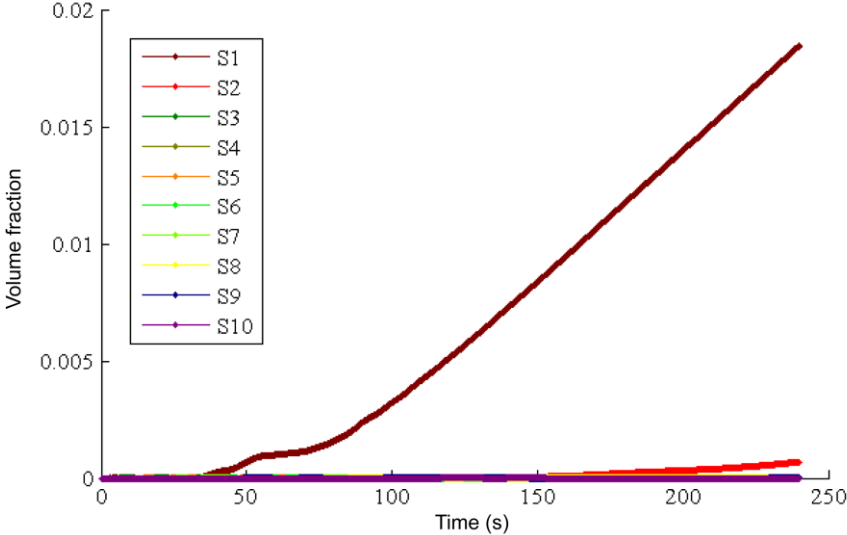
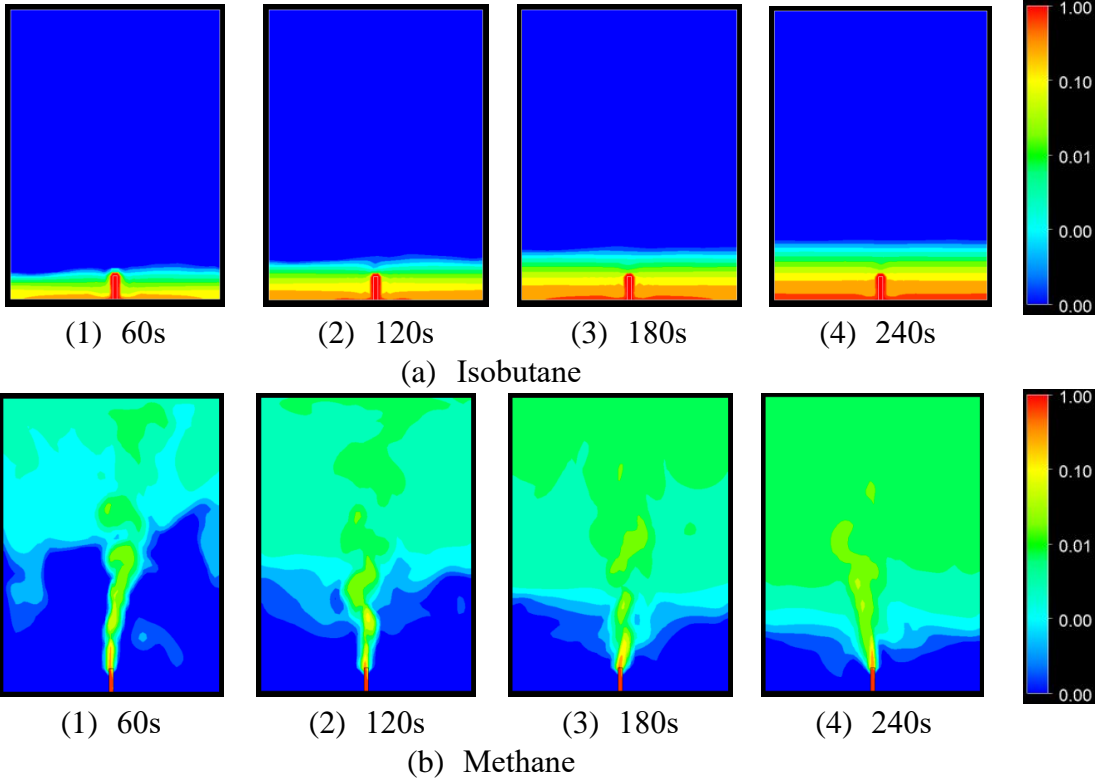
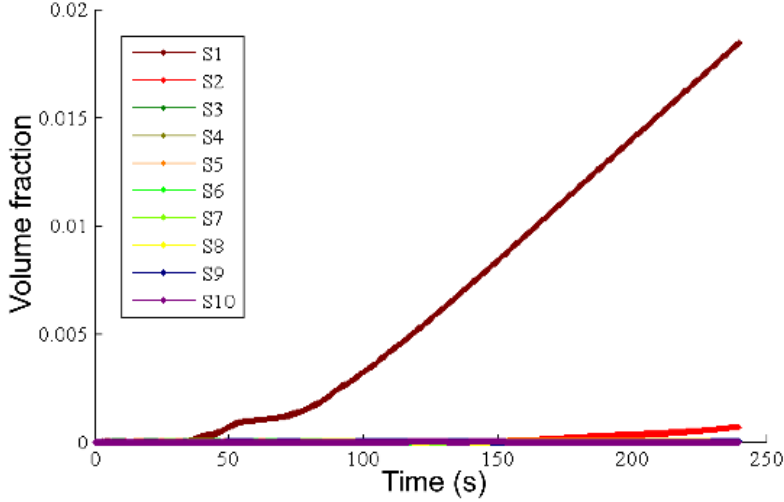


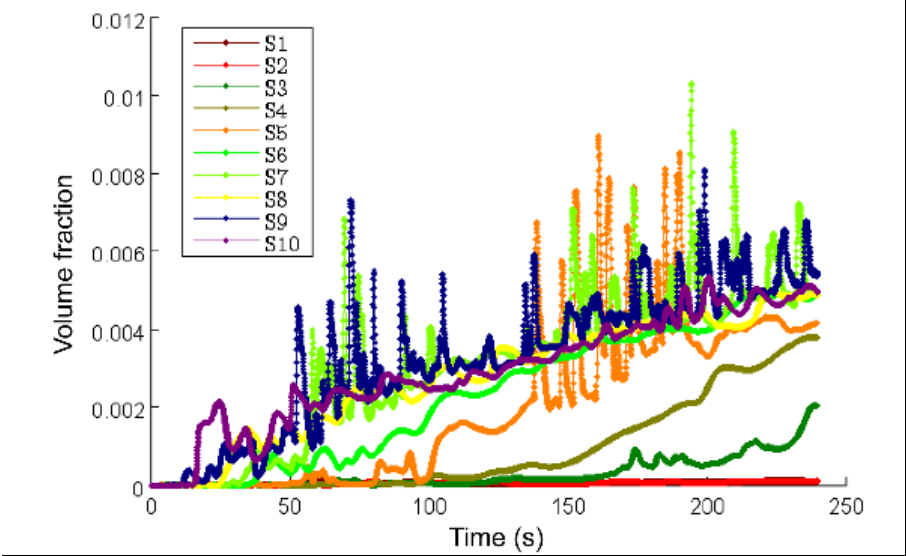
Fig.4. Contours of Volume Fraction of Various Components

Figure 5 shows the variation trend of the volume fraction of isobutane and methane at each observation point. It can be seen from Figure 5 (a) that the volume fraction of isobutane at the

bottom of the space increases linearly with time, and the gas volume fraction at the height of above 0.12m is close to zero and does not grow almost. From Figure 5 (b) it can be seen that methane is unstable in space, with a strong pulsation phenomenon. The volume fraction in the upper part of the space is large, and it is close to zero at the bottom.

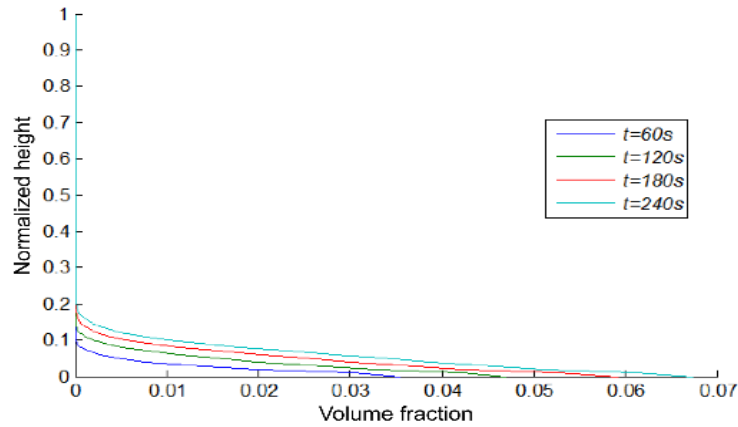


(a) Isobutane

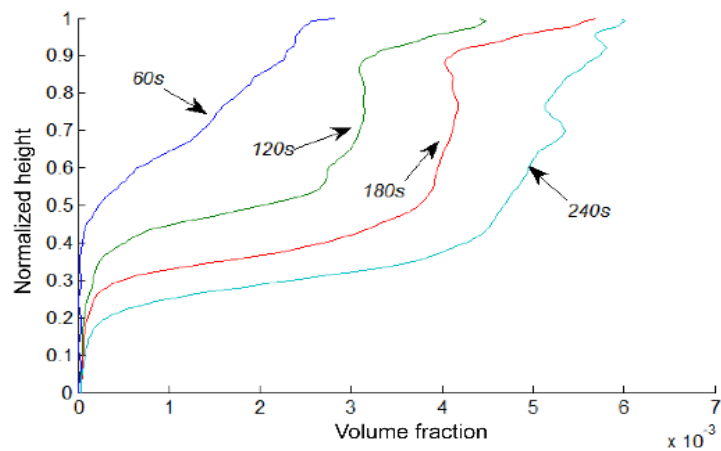


(b) Methane

Fig.5. Gas Volume Fraction on Moniting Points Vs Time



(a) isobutane



(b) methane

Fig.6. Vertical Distribution of Gas Volume Fraction After Leaking in 240s

To visually present the relative distribution features of the gas volume fraction in the space, the vertical position is normalized in the vertical direction (Figure 6). It can be seen from Fig. 6 (a) that isobutane has been occupying the lowest 20% of the space within 4 min warning time and has a larger volume fraction (up to 6.7%). It can be seen from Fig. 6 (b) that the methane gas rises rapidly and is dispersed in the upper part of the space. The distribution range increases rapidly with time and has been occupying the upper 80% of the space within 4 min.

In summary, the distribution rules of different components of the gasoline vapor after leakage show significant differences. The isobutane with density larger than the air (relative density is 2.07) first flows down, while the methane whose density is less than the air (relative density is 0.56) rises quickly and is evenly distributed in the upper space. In the safety monitoring of restricted spaces such as the actual depot, the gas alarm sensor should be installed in a lower position in the space to monitor the heavier gas in order to detect the leakage as soon as possible. At the same time, for lighter gases such as methane, the gas alarm sensor should be installed at the top of the space to

detect anomalies as early as possible. It is clear that if the leakage time is long enough (e.g. 30 min), the space will be evenly filled with the lighter component gas, and the heavier component gas will continue to rise from bottom to top (Figure 6a).

Conclusions

(1) In the simulation of gas plume using Large eddy simulation (LES), it is reasonable to ignore the flux terms of the mass fraction of the mass conservation equation which is filtered by the filter function, that is, no modeling is carried out to the flux of the sub-grid mass fraction.

(2) To ensure the validity of LES in the simulation of gas plume stratification characteristics, it is necessary to supplement and perfect the numerical simulation model, numerical format, meshing and time step.

(3) In the oil and gas mixture formed after the leakage of the fuel in the confined space, the light component (whose density is less than air) and the heavy component (whose density is greater than air) show a significantly different spatial distribution rule. Heavy components tend to accumulate in the lower part of the space, and the volume fraction is larger; the light components tend to be dispersed in the top of the space, and the volume fraction is small, but the distribution range is larger. Either light or heavy components all present a strong non-linear distribution.

(4) According to the research results of this paper, the reasonable arrangement of sensor is very important in the actual monitoring and early warning of the danger source such as the oil depot. This paper provides the key parameters and relevant engineering design basis accordingly.

Acknowledgments

Financial support for this work, provided by the National Natural Science Foundation of China (No. 21377166) and the National Key Research and Development Program of China (No. 2017YFC0804705), is gratefully acknowledged.

References

1. B. Cariteau, I. Tkatschenko, Experimental study of the concentration build-up regimes in an enclosure without ventilation, 2012, *International Journal of Hydrogen Energy*, vol. 37, no. 22, pp. 17400-17408.
2. G.R. Hunt, T.S.V.D. Bremer, Classical plume theory: 1937–2010 and beyond, 2011, *Ima Journal of Applied Mathematics*, vol. 76, no. 3, pp. 424-448.

3. M. Siddiqui, S. Jayanti, T. Swaminathan, CFD analysis of dense gas dispersion in indoor environment for risk assessment and risk mitigation, 2012, *Journal of Hazardous Materials*, vol. 209–210, no. 1, pp. 177-185.
4. G.G. Rooney, D.J. Thomson, Large-eddy simulation of a buoyant plume in uniform and stably stratified environments, 2010, *Journal of Fluid Mechanics*, vol. 652, no. 4, pp. 75-103.
5. L. Davidson, P.V. Nielsen, C. Topp, *Low-Reynolds number effects in ventilated rooms: A numerical study*, 2000, Pergamon Press.
6. R.Q. Wang, W.K. Law, E.E. Adams, O.B. Fringer, Large-eddy simulation of starting buoyant jets, 2011, *Environmental Fluid Mechanics*, vol. 11, no. 6, pp. 591-609.
7. S.E. Gant, *Quality and Reliability Issues with Large-Eddy Simulation*, 2009.
8. Y. Tominaga, T. Stathopoulos, Turbulent Schmidt numbers for CFD analysis with various types of flowfield, 2007, *Atmospheric Environment*, vol. 41, no. 37, pp. 8091-8099.
9. B.J. Guerts, *Elements of direct and large eddy simulation*, 2003.
10. J.H. Ferziger, M. Perić, *Computational Methods for Fluid Dynamics*, 1997, *Physics Today*, vol. 50, no. 3, pp. 80-84.
11. C. Germany, B. Smith, *CFD Best Practice Guidelines for CFD Code Validation for Reactor Safety Applications*, 2002, EC Project ECORA, Report EVOL-ECORA-D01.
12. B.M. Cetegen, K.D. Kasper, Experiments on the oscillatory behavior of buoyant plumes of helium and helium - air mixtures, 1996, *Physics of Fluids*, vol. 8, no. 11, pp. 2974-2984.
13. A.C.V.D. Berg, C.J.M.V. Wingerden, *Vapour cloud explosions: Experimental investigation of key parameters and blast modelling*, 1991, *Icheme Symposium Series*, No. 124, pp. 393-409.
14. K. Armstrong, *The new IET Guide – how to do EMC to help achieve Functional Safety*, 2010, Springer London, pp. 187-210.